AIP | Chaos
An Interdisciplinary Journal of Nonlinear Science

Chaotic behavior of light-assisted physical aging in arsenoselenide glasses

O. Shpotyuk, V. Balitska, A. Kozdras, A. S. Hacinliyan, Y. Skarlatos, I. Kusbeyzi Aybar, and O. O. Aybar

Citation: Chaos: An Interdisciplinary Journal of Nonlinear Science **24**, 043138 (2014); doi: 10.1063/1.4903795
View online: http://dx.doi.org/10.1063/1.4903795
View Table of Contents: http://scitation.aip.org/content/aip/journal/chaos/24/4?ver=pdfcov
Published by the AIP Publishing

Chaotic behavior of light-assisted physical aging in arsenoselenide glasses

O. Shpotyuk,[1,2,a)] V. Balitska,[1,3] A. Kozdras,[4] A. S. Hacinliyan,[5,6,7] Y. Skarlatos,[6] I. Kusbeyzi Aybar,[8] and O. O. Aybar[9]
[1]*Lviv Scientific Research Institute of Materials of SRC "Carat," 202, Stryjska Str., Lviv 79031, Ukraine*
[2]*Institute of Physics of Jan Dlugosz University, 13/15, al. Armii Krajowej, Czestochowa 42201, Poland*
[3]*Lviv State University of Vital Activity Safety, 35, Kleparivska str., Lviv 79007, Ukraine*
[4]*Opole University of Technology, 75, Ozimska str., Opole 45370, Poland*
[5]*Department of Physics, Yeditepe University, Atasehir 34755, Istanbul, Turkey*
[6]*Department of Physics, Bogazici University, Bebek, Istanbul, Turkey*
[7]*Department of Information Systems and Technologies, Yeditepe University, Atasehir 34755, Istanbul, Turkey*
[8]*Department of Computer Education and Instructional Technology, Yeditepe University, Atasehir 34755, Istanbul, Turkey*
[9]*Department of Mathematics, Faculty of Science and Letters, Piri Reis University, Tuzla 34940, Istanbul, Turkey*

(Received 12 June 2014; accepted 27 November 2014; published online 10 December 2014)

The theory of strange attractors is shown to be adequately applicable for analyzing the kinetics of light-assisted physical aging revealed in structural relaxation of Se-rich As-Se glasses below glass transition. Kinetics of enthalpy losses is used to determine the phase space reconstruction parameters. Observed chaotic behaviour (involving chaos and fractal consideration such as detrended fluctuation analysis, attractor identification using phase space representation, delay coordinates, mutual information, false nearest neighbours, etc.) reconstructed via the TISEAN program package is treated within a microstructure model describing multistage aging behaviour in arsenoselenide glasses. This simulation testifies that photoexposure acts as an initiating factor only at the beginning stage of physical aging, thus facilitating further atomic shrinkage of a glassy backbone. [http://dx.doi.org/10.1063/1.4903795]

Physical aging is one of the most diverse issues in the modern glass science. Being subjected to prolonged storage at the ambient conditions, the glasses lost their excess of configuration entropy, enthalpy or free volume to approach thermodynamic equilibrium. Light exposure with near-band-gap energy photons accelerates this process ending to quicker saturation. Observed non-linearity in the kinetics of light-assisted physical aging with character scoop-like spectral behaviour demonstrates an essential deterministic chaos as it was proved for binary arsenoselenide As-Se glasses using the TISEAN program package.

Physical picture of relevant structural transformations is thus clarified testifying that light exposure acts like initiating factor at the beginning stage of aging, facilitating twisting of Se atoms within double-well potentials of nearest atomic environment followed by global atomic shrinkage of a whole glassy backbone.

I. INTRODUCTION

Although high photosensitivity of chalcogenide glasses (ChG) has been known for a long time and many models have been proposed to explain this unique phenomenon in these disordered solids,[1–4] a little attention being paid to kinetics of structural changes, especially in respect to native metastability proper to such glass-forming systems.[5–9] Numerous investigations were focused on compositional trends of light-assisted physical aging (PhA) in ChG,[9–19] a specific type of below-T_g structural relaxation caused by sub-band-gap light exposure. Response magnitude was shown to depend on the light intensity, thermal prehistory of the samples and connectivity of glassy backbone.

One of most convenient ways to approach such problems in nonlinear disordered systems like ChG is to analyze the corresponding kinetics using a theory of *chaos*.[20–22] Recently, such an approach has been adequately applied to describe kinetics of natural PhA revealed in structural relaxation of Se-rich As-Se glasses below glass transition T_g.[23] Kinetics of enthalpy losses ΔH induced by prolonged storage in natural ambient conditions was used to determine the phase space reconstruction parameters, the emerged *chaoticity* was attributed to complex nature of underlying structural transformations initialized by multiply repeated mixed serial-parallel cycles of Se atoms twisting within double-well potentials of nearest chemical neighbours (aligning of Se chains) followed by atomic shrinkage at larger length scales.[24–28] In the present paper, this approach has been applied to disclose *deterministic chaoticity* in the kinetics of enthalpy losses in As-Se ChG under prolonged exposure by light of different discrete wavelengths.

II. EXPERIMENTAL

Glasses of As-Se system of four distinct compositions (g-$As_{10}Se_{90}$, g-$As_{20}Se_{80}$, g-$As_{30}Se_{70}$, and stoichiometric g-$As_{40}Se_{60}$) were prepared by known melt-quenching route in the evacuated quartz ampoules from a mixture of high purity precursors, as described elsewhere.[23–28] Amorphous state of glassy bulks were controlled visually by a characteristic conch-like fracture, as well as data of X-ray diffractometry.

[a)]Electronic address: shpotyuk@novas.lviv.ua

The prepared ChG samples in the form of plates (~3 mm in thickness) were analyzed with differential scanning calorimetry (DSC). Before experiments had started, all samples were rejuvenated by heating at ~40 K above corresponding onset values of the glass transition temperature T_g to erase any thermal prehistory. The cooling rate during this rejuvenation procedure was kept equal to the heating rate of the DSC measurements (5 K/min). Then, the identical batches of rejuvenated ChG samples were illuminated with continuous light of discrete wavelengths λ (430, 505, 590, 620, 660, 720, 780, and 970 nm) from light emitting diode (LED) sources (Roithner LaserTechnik GmbH, Austria), the width of half maximum of emission lines for each wavelength not exceeding ~50 nm. The power of every LED was chosen in such a way to keep constant photon flux for each wavelength (~2.5×10^{16} photons·cm^{-2} s^{-1}). It was controlled during a whole period of photo exposure by Optical Power Meter PM100A equipped with Thermal Power Head S302C. The applied chamber allowed temperature control and air convection to prevent spontaneous heating of the samples during illumination (no temperature deviations beyond 25 ± 2 °C range were detected during a whole period of PhA).

The ChG were tested with conventional DSC routine after certain time periods under photoexposure to register the kinetics curves of enthalpy recovery, assuming that the rejuvenated samples were quite close to as-prepared ones. We restricted our experiments with no more than 60 days of light illumination, when overall enthalpy losses were competitive with similar changes caused by long-term natural PhA (lasting more than two decades) in the same ChG samples.[9,27,28] This allows compare these effects by corresponding kinetics of enthalpy losses $\Delta H(t)$ taken at the equivalent number of measuring steps of different weights.

The DSC measurements were performed using NETZSCH 404/3/F microcalorimeter pre-calibrated with set of standard elements, the DSC patterns being recorded *ex-situ* in a dark at the ambient atmosphere with 5 K/min heating rate. The same calibration procedure was repeated each time during routinely kinetics recording. Three independent measurements were performed in each case to confirm the reproducibility of DSC results processed using NETZSCH PC software package. More detailed description of the experimental measuring procedure can be find elsewhere.[18,19]

The effect of light exposure was revealed by DSC technique as appearance of strong endothermic peak superimposed on the endothermic step of glass transition signal and its possible displacement towards higher temperatures.[17–19] The difference in the area under the DSC signal of light-soaked and rejuvenated ChG was directly proportional to the regaining of enthalpy ΔH lost during photoexposure and, consequently, used as a measure of "pure" light-assisted PhA.

III. RESULTS AND DISCUSSION

A. Comparison between real-time kinetics of light-assisted and natural PhA in As-Se glasses

The microstructure origin of natural PhA in Se-based ChG was shown to rely on local rearrangement of bridge chalcogen atoms occupying different configuration states which were described by double-well potentials of neighbouring environment, this chain-aligning process being followed by cooperative atomic shrinkage at more stretched length scales.[9,24,25] Three possible chemical environments for central Se atoms can be distinguished in binary As-Se glasses: Se-**Se**-Se fragments within Se_n chains (the number n of Se atoms in the chain is considered as the mean number of chalcogen atoms between As atoms), As-**Se**-Se and As-**Se**-As. The double-well potential associated with each of these fragments has different energetic barrier and local configuration parameters. Therefore, the activation energies for over-barrier transitions or tunneling of Se atoms between two neighboring states within such double-well potentials are different, giving variety of possibilities for expected external activation. Twisting of Se atoms within double-well potential of Se-**Se**-Se fragments is responsible for fast component in the natural PhA, while twisting of Se atoms within As-**Se**-Se fragments (followed by shrinkage of under-constrained glassy network having less than three Lagrangian constraints per atom[9]) are shown to have more prolonged kinetics of structural relaxation.[24–28] In contrast, the rearrangements of Se atoms within As-**Se**-As fragments which are main building blocks of stoichiometric As_2Se_3 glass are hardly possible at all because of low probability of corresponding over-barrier tunneling. So having been subjected to very long natural PhA during more than two decades, this As_2Se_3 glass demonstrates excellent non-aging ability (in exception to enhanced temperatures, when over-barrier rearrangements became possible owing to thermally-activated mechanisms).[9]

The light-assisted PhA in the studied ChG can be associated with similar mechanisms as those characterizing natural PhA,[9,24–28] the only difference being in the initiating factors for structural relaxation. During natural PhA, the elementary relaxations of Se atoms within double-well potentials associated with Se-**Se**-Se and As-**Se**-Se fragments have a fluctuation nature. Randomly started at different sites in a sample bulk, they initiate further shrinkage of a glassy network due to contraction of free-volume spaces released during twisting (or alignment) of Se polymeric chains. In case of light-assisted PhA, these processes can be facilitated via direct and indirect inter-band transitions associated with bond breaking or switching, formation of valence alternation pairs, thermalization of the excited electrons, inelastic photon scattering, phonon-assistant transitions or two-photon absorption, each of these processes being significantly dependent on the choice of chalcogen atom.[9,18] Therefore, like natural PhA, the light-assisted PhA in As-Se glasses decays significantly with As content, so in stoichiometric $As_{40}Se_{60}$ this effect is absent and in $As_{30}Se_{70}$ glass it attains only under-margin negligible amplitude. Thus, reliable DSC measurements can be performed only for other two Se-rich samples in this cut-section, the $As_{10}Se_{90}$ and $As_{20}Se_{80}$. Kinetics dependencies of enthalpy losses ΔH in these glasses caused by photoexposure of different wavelengths λ are shown in a semi-logarithmic scale in Figure 1.[18,19]

These kinetics curves are quite similar to ones character for long-term natural PhA in the same ChG[27,28] in spite of obvious difference in the overall aging duration. The maximal value of enthalpy losses ΔH which can be reached in

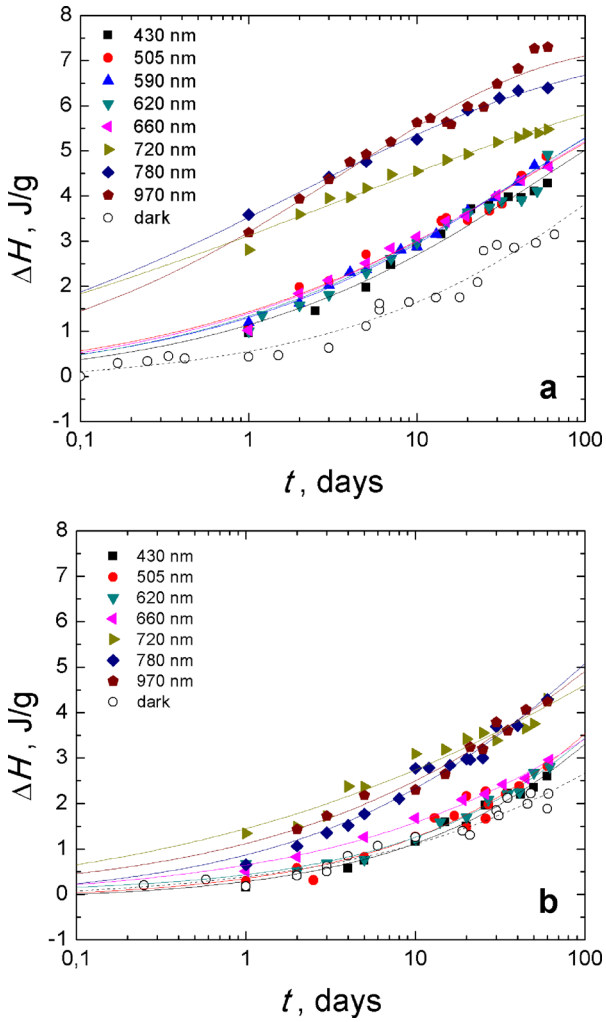

FIG. 1. Real-time kinetics of light-assisted (colored symbols) and natural (open symbols) PhA in glassy $As_{10}Se_{90}$ (a) and $As_{20}Se_{80}$ (b).

$As_{10}Se_{90}$ and $As_{20}Se_{80}$ glasses after two-months photoexposure with 970 nm wavelength are 7.3 and 4.2 J/g, respectively, (in long-term aged samples, the corresponding ΔH values are 7.1 and 6.2 J/g, respectively).[9,23] But, in contrast to natural PhA displaying an obvious multistep-wise behavior,[27,28] these are typically growing curves for both $As_{10}Se_{90}$ and $As_{20}Se_{80}$ glasses showing more or less smooth increase in the enthalpy losses ΔH with illumination time t and only slight step-like deviations during a whole photoexposure.

It is noteworthy that all kinetics curves on $\Delta H(t)$ plot are grouped along two character positions, the first (the higher) being affected by well-penetrating under-band-gap light and second (the lower) being caused by band-gap and over-band-gap light which is more absorbed by bulk ChG samples. The kinetics of dark-aged glass is closer to one corresponding to light-assisted PhA with band-gap and over-band-gap light.

Thus, despite common tendencies in the generalization trend of PhA tending ChG system towards thermodynamic equilibrium (growing behavior in the enthalpy losses ΔH), a light-assisted process of enthalpy recovery shows remarkable difference in respect to its wavelength dependence. The bifurcation in set of ΔH values distinguished by optical band gap was never defined for natural processes of PhA, which are rather affected by preference of unified growing tendency. A great variety of initiating processes leading to light-assisted enthalpy growing ΔH in ChG[18,19] puts an important question on the universality of their phenomenology, like that developed within a formalism of potential energy landscape for network glass formers.[29–32]

B. Chaotic behavior in the kinetics of light-assisted PhA in As-Se glass

In this section, the light-assisted PhA in As-Se glass will be analyzed in respect to the applied time series method[20–22] using TISEAN program package,[33,34] which allow *chaos* and *fractal analysis* such as *attractor reconstruction* due to *phase space* representation, *delay coordinates*, *mutual information*, *false nearest neighbors* (henceforth referred to as FNN), and *detrended fluctuation analysis* (henceforth referred to as DFA).

C. DSC enthalpy losses *vs.* time graphs

We observe irregular transient enthalpy losses ΔH for studied ChG samples under light-assisted PhA as shown above in Fig. 1. One net way to understand this non-linearity is to take increasing enthalpy losses ΔH as a slowly varying parameter with data split into equal time domains. After splitting, the delay times are analyzed using the delay-coordinate embedding theorem.[21,35] If the embedding is performed correctly, the theorem guarantees that the reconstructed dynamics of the system should be identical to true dynamics and dynamical invariants should also be identical. To work on time series at first, we build up the delay vectors $x(T)$, $x(T+t)$,…., $x(T+(m-1)t)$. Here, t and m represents delay time and embedding dimension, respectively. The reconstructed invariants (basically, its fractal dimensions) of the attractor as found by this approach remain invariant with respect to unknown, original system that generated the series.

Figures 2(a) and 2(b) show reconstructed kinetics of light-assisted PhA spitted into equal time domains in $As_{10}Se_{90}$ and $As_{20}Se_{80}$ glasses, respectively. In a linear scale, these curves show sharp initial growing followed by more stretched ΔH saturation. As in the case of real-time kinetics in Figure 1, these are also grouped near two positions, the stronger being affected by under-band-gap light, while the weaker being produced by band-gap and under-ban-gap light.

D. Mutual information

In contrast to linear dependence measured by autocorrelation, *the mutual information I(t)*, serves as an indicator of general dependence providing a better measure for transition from small to large times t within a chosen nonlinear system.[23]

The mutual information $I(t)$ defines the smallest figure which ensure prediction of observation $S(T+t)$ after delay of time t, starting from given observation $S(T)$ at time T, so that successive delay coordinates can be interpreted as relatively independent.[36] Within the TISEAN program,[29,34] the value of time delay where $I(t)$ reaches first minimum is used for space reconstruction.

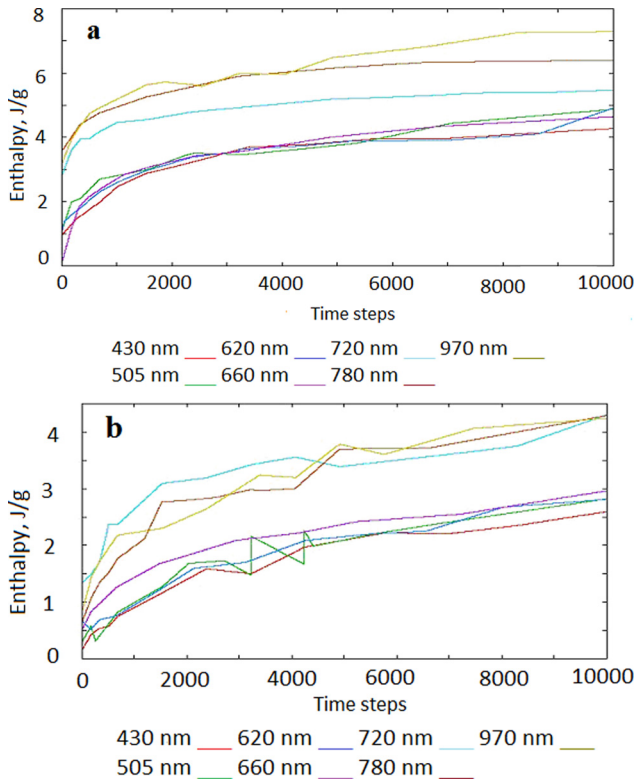

FIG. 2. Reconstructed DSC enthalpy losses *vs.* time graphs for light-assisted PhA induced by different wavelengths in glassy $As_{10}Se_{90}$ (a) and $As_{20}Se_{80}$ (b).

The main procedure is based on two sets X and Y with x_i being the possible outcome of a measurement on X and y_j being the possible outcome of a measurement on Y. It is obvious that if the measurement x_i is independent from y_j then the following condition is satisfied:

$$P_{XY}(x_i; y_i) = P(x_i)P(y_i). \tag{1}$$

The joint probability of observing x_i and y_j is different if there exists correlation between the two outcomes. Average mutual information of X and Y defined as the logarithm of ratio in bits is

$$\log_2 \frac{P_{XY}(x_i; y_i)}{P(x_i)P(y_i)}. \tag{2}$$

Thus, the weighted average of mutual information can be defined as

$$I(X;Y) = -\sum_x \sum_y P_{XY}(x_i; y_i) \cdot \log_2 \frac{P_{XY}(x_i; y_i)}{P(x_i)P(y_i)}. \tag{3}$$

When this is applied to a time series $S(n)$, the following new formula is obtained:

$$I(t) = -\sum_x \sum_y P\big(s(n+t), s(n)\big) \cdot \log_2 \frac{P\big(s(n+t), s(n)\big)}{P(s(n+t)) \cdot P(s(n))}. \tag{4}$$

This approach applied to long-term natural PhA in Se-rich g-As-Se (g-$As_{10}Se_{90}$, g-$As_{20}Se_{80}$, and g-$As_{20}Se_{80}$) gives time delay t of approximately ~250 steps despite glass composition. This specificity was explained by preferential input of the same structural entities responsible for primary changes causing natural PhA. In respect to previous microstructure study,[24,25] these aging-related processes are identified as twisting of inner Se atoms within heteropolar environment of double-well potentials (mainly As-**Se**-Se fragments). The mutual information $I(t)$ *vs.* delay time t graphs for glassy $As_{10}Se_{90}$ and $As_{20}Se_{80}$ subjected to light-assisted PhA are given in Figures 3(a) and 3(b), respectively.

It is clear that when we analyze the light-assisted PhA with respect to the wavelengths of photoexposure, the delay time in $As_{10}Se_{90}$ glass varies considerably from 200 to 300 time steps, this is comparable to the averaged value for natural PhA (~250 time steps).[23] In case of $As_{20}Se_{80}$ glass, the delay time varies from 100 to 250 time steps with respect to the wavelengths of photoexposure, giving a somewhat reduced average value near ~180–200 time steps. So photoexposure does not significantly change delay times t determined in time steps in respect to those character for natural PhA (despite obvious difference in the weight of each step). This finding probably testifies in a favour of unified initiating stage facilitating structural recovery whichever its origin (natural or light-assisted PhA revealed in nearly the same amplitude of enthalpy losses ΔH).

E. Embedding dimension

To identify deterministic chaos in the behavior of nonlinear system, the phase reconstruction procedure should be

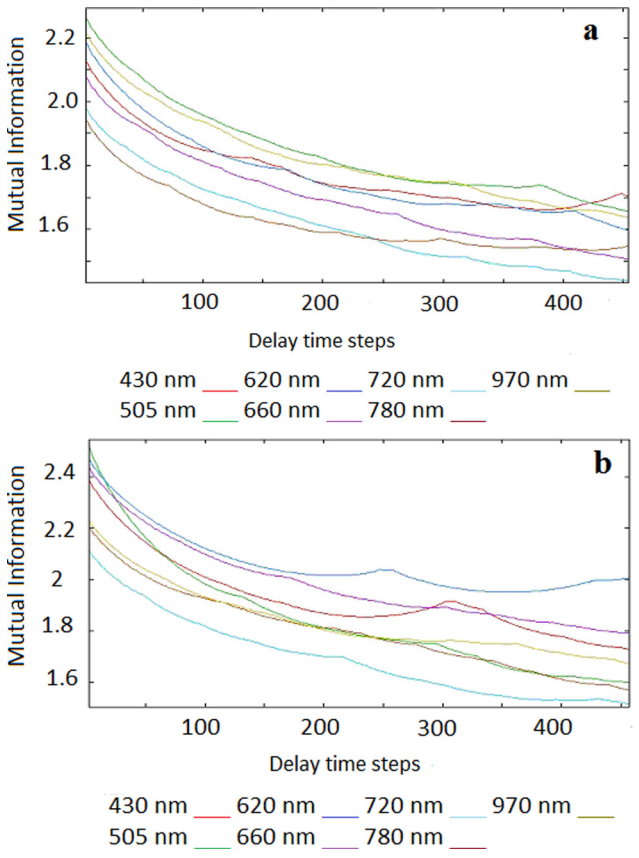

FIG. 3. Average mutual information *vs.* delay time graphs for light-assisted PhA in glassy $As_{10}Se_{90}$ (a) and $As_{20}Se_{80}$ (b).

performed adequately on a set of points forming a *strange attractor*.[35,36]

After choosing an acceptable time delay t, we need a sufficiently large embedding dimension m to reconstruct correctly the phase space, so to avoid projecting the system onto a lower dimensional space. In other words, we need a criterion for the minimum embedding dimension, sufficient to unfold the strange attractor. At this point, *the FNN method*[36] is useful tool to give an estimate for the embedding dimension m.

This method uses the property of the attractor which guarantees that there are no two orbits that intersect each other. For the desired embedded dimension m, we should have *fraction of FNN* that is close to zero within some tolerance. With this concept as an algorithm, one would start from small m values and calculate the generated number of false neighbors. One would then increase the number of dimensions m one by one until the number of false neighbors is nearly zero up to a tolerance that depends on artifacts such as observational error or noise. The number of dimensions m in which the number of false nearest neighbors becomes minimum and remains there as m is increased is the best embedding for the chosen nonlinear system (with the smallest number of dimensions required to correctly represent the system).

The methodology uses the reconstructed data vectors in m dimensions with a suitable time lag t and time-delay vector given as

$$y(k) = [S_k, S_{k+T}, ..., S_{k+(m-1)t}] \tag{5}$$

for $y \in R^m$, m being embedding dimension. In the embedded space, $y(k)$ and $y_{NN}(k)$ are neighbors in the embedded system. When embedding dimension is not large enough, the attractor does not unfold properly in the embedded space, so false neighbors collapse.

Distance between neighboring points in real embedded m dimension space is

$$R_m^2 = \|y(k) - y_{NN}(k)\|^2 = \\ = [[S_{NN(k)} - S_{(k)}]^2 + ... + [S_{NN(k+(m-1)t)} - S_{(k+(m-1)t)}]^2]. \tag{6}$$

In $m+1$ dimensions, the distance between neighboring points is

$$R_{m+1}^2(k) = R_m^2(k) + (S_{NN(k+(m)t)} - S_{(k+(m)t)})^2. \tag{7}$$

By using this, the threshold value $R_T(k)$ can be defined as

$$\frac{(S_{NN(k+(m)t)} - S_{(k+(m)t)})}{R_m(k)} > R_T(k). \tag{8}$$

Points that satisfy this threshold value become neighbors in m dimensions, but not neighbors in $m+1$ dimension.

By taking the delay time as given Sec. II D, we analyzed the minimum embedding dimension m needed to reconstruct the attractor by FNN method for light-soaked $As_{10}Se_{90}$ and $As_{20}Se_{80}$ glasses as given in Figures 4(a) and 4(b), respectively.

The light-assisted PhA concerns some deviation in the inner structure of glassy $As_{10}Se_{90}$ starting from bigger embedding dimensions to smaller ones as wavelength λ grows from 430 to 970 nm (see Figure 4(a)), so revealing a characteristic scoop-like spectral behavior. By supposing that phase space reconstruction is carried out in a sufficiently large number of embedding dimensions m, there will be no FNN and attractor will be unfolded in greater than or equal to these m dimensions.

From this point, some incorrectness remains for FNN in $As_{10}Se_{90}$ glass affected by light with $\lambda = 430$ and 970 nm. The corresponding curves demonstrate obvious remainders over FNN = 0 in a stationary regime, that is probably related to incompleteness in the PhA kinetics. In other words, the fraction of FNN in these samples sharply drops down at the first initial stage, tending slowly to full disappearance (if only) at higher embedding dimensions m. So it is reasonable to characterize such behavior with m value corresponding to initial sharpest decrease in the FNN. It means that embedding dimension m for $As_{10}Se_{90}$ glass photosoaked with $\lambda = 430$ and 970 nm can be accepted as $m = 4$, the value which is characteristic for natural PhA in this glass.[23]

Then, the embedding dimension starts to decrease to $m = 2$ as λ approaches the absorption edge of $As_{10}Se_{90}$ glass (near 620–720 nm). Thus, the light-assisted PhA in $As_{10}Se_{90}$ glass affected by near-band-gap light is attributed with minimal embedding dimension m close to 2.

For light-assisted PhA in $As_{20}Se_{80}$ glass (possessing $m = 3$ for long-term dark natural PhA in a dark[23]), the embedding dimensions m behave with wavelengths λ showing similar scoop-like trend (see Fig. 4(b)). First, the m reaches 3 at $\lambda = 430$ nm (by deducing the background

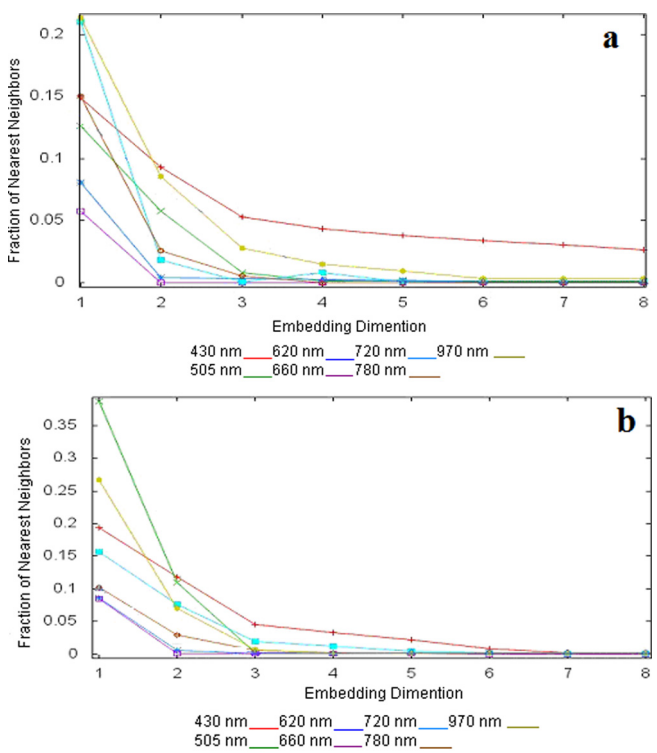

FIG. 4. Fraction of FNN *vs.* embedding dimension m for light-assisted PhA in glassy $As_{10}Se_{90}$ (a) and $As_{20}Se_{80}$ (b).

remainder in Fig. 4(b)), then it drops to $m=2$ for λ close to absorption edge ($\lambda=620$–720 nm), and afterwards it returns to $m\approx3$ with $\lambda=970$ nm (the only exception is for glass illuminated with $\lambda=720$ nm, which demonstrates some tendency towards bifurcation in m on sharp and slow parts).

In case of long-term natural PhA, the compositional deviations in the embedding dimensions m correlates well with smoothing tendency in the aging kinetics, when multiple step-wise trends observed in Se-rich arsenoselenide As-Se glasses (such as glassy $As_{10}Se_{90}$) become smoother in ChG with less Se content (like $As_{20}Se_{80}$ and $As_{30}Se_{70}$).[23] With this in mind, the observed spectral scoop-like trend in the embedding dimensions m for light-assisted PhA in these ChG corresponds strongly to the decreased diversity in the microstructure processes occurring as photon energy approaches the band-gap value. It can be supposed that close-to-bandgap light facilitate some stages of PhA (probably, the initiating stages of Se chains aligning), tending the overall process of PhA towards it quicker saturation.

From other point, when incident photons approach bandgap energy, an additional channel of structural relaxation appears to be possible in ChG.[19] This channel is connected with photoinduced defect formation in glassy material giving a distinct path to accommodate an abundant elastic stress (enthalpy recovery) during relaxation. So within Phillip's axiomatic diffusion-to-trap model,[37] we expect three different channels for relaxation under close-to-bandgap light illumination instead of two channels for above- and below-bandgap light. In all cases, only one of these channels, is effective for structural relaxation giving non-exponentionality index $\beta\cong0.3$ in stretched exponential kinetics of light-assisted PhA.[19] Under glass relaxation in a dark,[27,28] as well as under above- or below-bandgap photoexposure,[17–19] this kinetics tends to be stretched exponential with higher β index approaching 3/7 (or 0.43), the characteristic value caused by activation either of long-range or short-range interactions.[37–41] Remarkably, the observed scoop-like spectral behavior in the embedding dimension m corresponding to the reconstructed phase space for light-assisted PhA in the studied ChG correlates well with dropping tendency in non-exponentionality index β describing smoothing of the final relaxation kinetics.

The microstructural mechanism of PhA explains well observed stretch-exponential behavior in the relaxation kinetics in terms of hierarchically constrained mixed serial-parallel events, having different precursors (chemical environment around Se atoms) in dependence on ChG composition.[28] PhA dynamics for each chemical environment exhibits two-step scenario like in glassy polymers of the same molecular weight,[42–44] where the faster relaxation events are initiated by preferentially single-particle motions (responsible for aligning of neighbored Se chains), while the slower relaxation events are based on many-particle cooperative process (such as atomic shrinkage). These fast and slow relaxation stages are hierarchically arranged for each atomic precursor (the slower processes start after the faster ones are completed) within the glass network. We believe these hierarchically dependent processes have different effective time-constants and dispersivity as being initiated by Se-**Se**-Se or Se-**Se**-As precursors in As-Se glasses, forming more or less independent channels of structural relaxation. Strong correlations between non-exponentionality index β describing stretched exponential relaxation kinetics of light-assisted PhA and embedding dimensions m testifies that bandgap illumination removes partially the uncertainty of the system, while enhances the non-exponentionality in the relaxation kinetics.

F. Scaling analysis of power-low correlation exponent

This analytical procedure is aimed to clarify the system's behavior in phase space. Recently, some major studies on this issue were published by Marwan *et al.*[45] covering recurrence based methods and their application for complex systems. The reliable method for constructing a directed weighted complex network from a time series of chaotic dynamics was proposed by Gao *et al.*[46] Gao *et al.*[47] also designed a new multisector conductance sensor for measuring multivariate signals of different flow patterns for complex interacting components from a network perspective. Kantelhardta *et al.*[48] developed a method for multifractal characterization of nonstationary time series based on a generalization of the DFA to compare the proposed multifractal DFA to the standard partition function-based multifractal formalism. Recently, Gao *et al.*[49] used a framework of multivariate recurrence network to construct a network from multivariate signals.

In our research, to analyze short- and long-range correlations in the studied ChG accompanied light-assisted PhA, the DFA method was applied.[33] In fact, this method is *scaling analysis* to estimate so-called long-range power-law correlation exponent. One integrates the time series of length N, then divides the result into boxes of equal length n. In each box of length n, a least squares line is fit to the data. Next, the integrated time series is detrended by subtracting some local trend in each box and root-mean-square fluctuations $F(n)$ of this integrated and detrended time series are calculated. This computation is repeated over all time scales (box sizes) to characterize the relationship between average fluctuation $F(n)$ as a function of box size n. A linear relationship on log-log plot indicates power-law scaling. Under such consideration, the fluctuations can be characterized by scaling exponent α, such that $F(n):n^{\alpha}$. The crossover in the scaling type of underlying correlation can be attributed to possible transition in the dynamical properties.[50–54]

In case of natural PhA in g-As-Se,[23] the DFA shows similar properties concerning more than one regime at the beginning and come closer to be within the same regime at the end of PhA. Thus, the starting stages of natural PhA in glassy $As_{10}Se_{90}$ and $As_{20}Se_{80}$ has similar characteristics with slope of 1.57, changing this slope towards 1.90 with further stages, which occurs to be also the slope for natural PhA in $As_{30}Se_{70}$ glass.

According to our analysis (see Figure 5), the samples of glassy $As_{10}Se_{90}$ and $As_{20}Se_{80}$ affected by light-assisted PhA at different wavelengths have similar DFA regimes. Therefore, we can suggest that when these ChG are under light-assisted PhA, they behave like under natural PhA in a

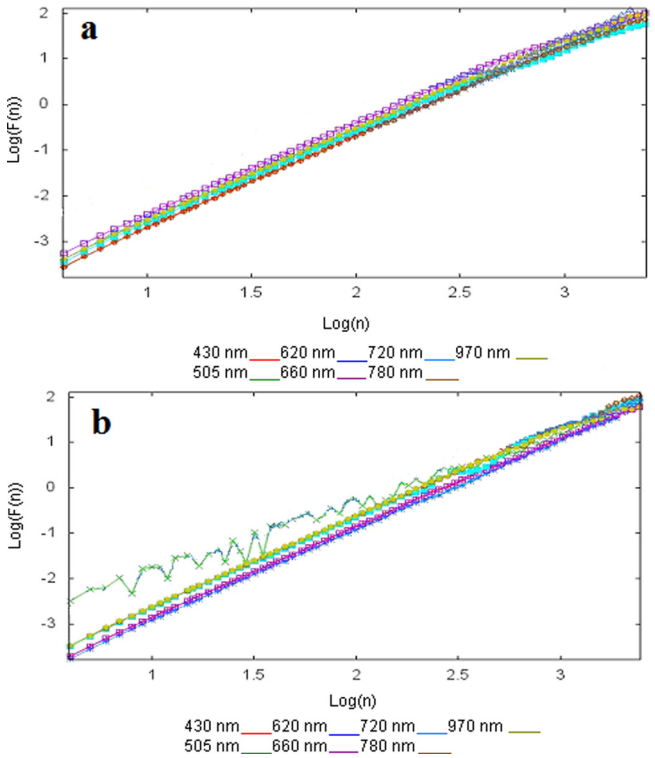

FIG. 5. DFA graphs for light-assisted PhA in glassy $As_{10}Se_{90}$ (a) and $As_{20}Se_{80}$ (b).

dark after sufficiently prolonged time period, as it can been observed, for example, in long-term natural PhA of $As_{30}Se_{70}$ glass.[23] It means that photoexposure acts as initiating factor only at the beginning stage of below-T_g structural relaxation, probably activating twisting of Se atoms within double-well potential configurations of their nearest chemical environment (Se-**Se**-Se and Se-**Se**-As chain-like fragments), thus significantly facilitating initial stage of PhA. So the final atomic shrinkage remains the same (as in the case of long-term natural PhA), whichever original reason for below-T_g structural relaxation (natural storage at ambient conditions, thermal heating, light exposure, or even high-energy irradiation, etc.).

IV. CONCLUSION

In conclusion, when we analyze spectral dependence of light-assisted PhA, the delay time varies considerably within 200–300 time steps in $As_{10}Se_{90}$ and 100–250 time steps in $As_{20}Se_{80}$ glasses, testifying in a favour of some similarities with natural PhA. The light-assisted PhA concerns some transformations in the inner structure of ChG starting from bigger embedding dimensions to smaller ones character for naturally aged samples as wavelength varies towards close-to-bandgap values, so obviously revealing character scoop-like spectral dependence. In respect to detrended fluctuation analysis, we can suggest that when samples are under light influence, they behave like under natural PhA in sufficiently long-term period. It means that light exposure acts as initiating factor at the beginning stage of PhA, e.g., twisting of Se atoms within double-well potentials of nearest chemical environment. The finalizing atomic shrinkage remains the same as in the case of prolonged natural PhA, whichever original reason for below-T_g structural relaxation.

ACKNOWLEDGMENTS

The authors acknowledge thanks to TUBITAK "The Scientific and Technical Research Council of Turkey" under the project number "111T805" and DKNII "The State Agency of Ukraine for Science, Innovation and Information Technology" for initiating international collaboration and providing financial support for this research. This study is partially supported by the Bogazici University Research Fund.

[1]A. V. Kolobov, *Photo-induced Meta-stability in Amorphous Semiconductors* (Wiley-VCH, Weinheim, 2003).
[2]K. Tanaka, A. Saitoh, and N. Terakado, "Photoinduced phenomena in group VIb glasses," J. Mater. Sci.: Mater. Electron. **20**, Supplement, 38 (2009).
[3]M. Frumar, M. Vlcek, Z. Cernosek, Z. Polak, and T. Wagner, "Photoinduced changes of the structure and physical properties of amorphous chalcogenides," J. Non-Cryst. Solids **213–214**, 215 (1997).
[4]K. Shimakawa, A. Kolobov, and S. R. Elliott, "Photoinduced effects and metastability in amorphous semiconductors and insulators," Adv. Phys. **44**, 475 (1995).
[5]L. C. E. Struik, *Physical Aging in Amorphous Polymers and Other Materials* (Elsevier, New York, 1978).
[6]A. Feltz, *Amorphous Inorganic Materials and Glasses* (VCH, Weinheim, 1993).
[7]J. M. Saiter, M. Arnoult, and J. Grenet, "Very long physical aging in inorganic polymers emplied by the Ge_xSe_{1-x} vitreous system," Physica B **355**, 370 (2005).
[8]S. H. M. Shieh and W. C. LaCourse, "Aging and sub-T_g relaxation in arsenic selenide glass fibers," Mater. Chem. Phys. **35**, 160 (1993).
[9]O. Shpotyuk, R. Golovchak, and A. Kozdras, "Physical aging of chalcogenide glasses," in *Chalcogenide Glasses: Preparation, Properties and Applications*, edited by J.-L. Adam and X. Zhang (Woodhead Publishing Series in Electronics and Optical Materials, Philadelphia-New Delhi, 2013).
[10]J. P. Larmagnac, J. Grenet, and P. Michon, "Photodependence of sub-T_g relaxation in a-Se thin films," Philos. Mag. B **45**(6), 627 (1982).
[11]D. J. McEnroe and W. C. LaCourse, "Tensile strengths of Se, As_2S_3, As_2Se_3, and $Ge_{30}As_{15}Se_{55}$ glass fibers," J. Am. Ceram. Soc. **72**, 1491 (1989).
[12]C. Vautier, T. Derrey, J. M. Saiter, and Ph. Lebaudy, "Photorelaxation in amorphous Ge_xSe_{1-x} $(0 < x < 0.08)$ thin films," J. Non-Cryst. Solids **131–133**, 520 (1991).
[13]P. Lucas, E. A. King, A. Doraiswamy, and P. Jivaganont, "Competitive photostructural effects in Ge-Se glass," Phys. Rev. B **71**, 104207 (2005).
[14]P. Lucas, "Energy landscape and photoinduced structural changes in chalcogenide glasses," J. Phys.: Condensed Matter **18**, 5629 (2006).
[15]P. Lucas, E. A. King, A. D. Horner, B. R. Johnson, and S. K. Sundaram, "Photostructural relaxation in As-Se-S glasses: effect of network fragility," J. Non-Cryst. Solids **352**, 2067 (2006).
[16]L. Calvez, Zh. Yang, and P. Lucas, "Light-induced matrix softening of Ge-As-Se network glasses," Phys. Rev. Lett. **101**, 177402 (2008).
[17]R. Golovchak, A. Kozdras, and O. Shpotyuk, "Physical aging in glassy As-Se induced by above-bandgap photoexposure," Solid State Commun. **145**, 423 (2008).
[18]A. Kozdras, R. Golovchak, O. Shpotyuk, S. Szymura, A. Saiter, and J.-M. Saiter, "Light-assisted physical aging in chalcogenide glasses: dependence on the wavelength of incident photons," J. Mater. Res. **26**, 2420 (2011).
[19]R. Golovchak, A. Kozdras, and O. Shpotyuk, "Kinetics of light-assisted physical aging in chalcogenide glasses," J. Mater. Sci. **49**, 2844 (2014).
[20]H. Kantz and T. Schreiber, *Nonlinear Time Series Analysis* (Cambridge University Press, Cambridge, 2003).
[21]H. D. I. Abarbanel, R. Brown, J. J. Sidorowich, and L. Sh. Tsimring, "The analysis of observed chaotic data in physical systems," Rev. Mod. Phys. **65**, 1331 (1993).
[22]T. Schreiber, "Interdisciplinary application of nonlinear time series methods," Phys. Rep. **308**, 1 (1999).

[23]A. S. Hacinliyan, Y. Skarlatos, I. Kusbeyzi Aybar, O. O. Aybar, O. Shpotyuk, R. Golovchak, V. Balitska, and A. Kozdras, "Natural physical aging in glassy As-Se: A comparative study of chaotic behaviour with enhanced results analysis," J. Non-Cryst. Solids **386**, 8 (2014).
[24]R. Golovchak, O. Shpotyuk, A. Kozdras, B. Bereau, M. Vlcek, A. Ganjoo, and H. Jain, "Atomistic model of physical aging in Se-rich As–Se glasses," Philos. Mag. **87**, 4323 (2007).
[25]R. Golovchak, O. Shpotyuk, A. Kozdras, M. Vlcek, B. Bureau, A. Kovalskiy, and H. Jain, "Long-term physical aging in As-Se glasses with short chalcogen chains," J. Phys.: Condensed Matter **20**, 245101 (2008).
[26]R. Golovchak, A. Ingram, A. Kozdras, M. Vlcek, C. Roiland, B. Bureau, and O. Shpotyuk, "Initial stage of physical aging in network glasses," Philos. Mag. **92**, 4182 (2012).
[27]R. Golovchak, A. Kozdras, V. Balitska, and O. Shpotyuk, "Step-wise kinetics of natural physical aging in arsenic selenide glasses," J. Phys.: Cond. Matter **24**, 505106 (2012).
[28]V. Balitska, R. Golovchak, A. Kozdras, and O. Shpotyuk, "Fine kinetics of natural physical aging in glassy $As_{10}Se_{90}$," Phys. B **434**, 21 (2014).
[29]M. Goldstein, "Viscous liquids and the glass transition: a potential energy barrier picture," J. Chem. Phys. **51**, 3728 (1969).
[30]F. H. Stillinger, "A topographic view of supercooled liquids and glass formation," Science **267**, 1935 (1995).
[31]A. Heuer, "Exploring the potential energy landscape of glass-forming systems: from inherent structures via metabasins to macroscopic transport," J. Phys.: Condensed Matter **20**, 373101 (2008).
[32]R. Golovchak, A. Kovalskiy, O. Shpotyuk, and H. Jain, "In search of energy landscape for network glasses," Appl. Phys. Lett. **98**, 171905 (2011).
[33]R. Hegger, H. Kantz, and T. Schreiber, "Practical implementation of nonlinear time series methods: The TISEAN package," Chaos **9**, 413 (1999).
[34]H. Kantz, "A robust method to estimate the maximal Lyapunov exponent of a time series," Phys. Lett. A **185**, 77 (1994).
[35]F. Takens, *Detecting strange attractors in turbulence*, Lecture Notes in Mathematics Vol. 898 (Springer-Verlag, New-York, 1981).
[36]T. Sauer, J. Yorke, and M. Casdagli, "Embedology," J. Stat. Phys. **65**, 579 (1991).
[37]J. C. Phillips, "Stretched exponential relaxation in molecular and electronic glasses," Rep. Progr. Phys. **59**, 1133 (1996).
[38]J. R. Macdonald and J. R. Phillips, "Topological derivation of shape exponents for stretched exponential relaxation," J. Chem. Phys. **122**, 074510 (2005).
[39]R. Bohmer and C. A. Angell, "Correlations of nonexponentiality and state dependence of relaxations with bond connectivity in Ge-As-Se supercooled liquids," Phys. Rev. B **45**, 10091 (1992).
[40]R. C. Welch, J. R. Smith, M. Potuzak, X. Guo, B. F. Bowden, T. J. Kiczenski, D. C. Allan, E. A. King, A. J. Ellison, and J. C. Mauro, "Dynamics of glass relaxation at room temperature," Phys. Rev. Lett. **110**, 265901 (2013).
[41]G. G. Naumis and J. C. Phillips, "Bifurcation of stretched exponential relaxation in microscopically homogeneous glasses," J. Non-Cryst. Solids **358**, 893 (2012).
[42]D. Cangialosi, "Dynamics and thermodynamics of polymer glasses," J. Phys.: Condensed Matter **26**, 153101 (2014).
[43]D. Cangialosi, V. M. Boucher, A. Alegria, and J. Colmenero, "Direct evidence of two equilibration mechanisms in glassy polymers," Phys. Rev. Lett. **111**, 095701 (2013).
[44]V. M. Boucher, D. Cangialosi, A. Alegria, and J. Colmenero, "Enthalpy recovery of glassy polymers: dramatic deviations from the extrapolated liquidlike behavior," Macromolecules **44**, 8333 (2011).
[45]N. Marwan, M. C. Romano, M. Thiel, and J. Kurths, "Recurrence plots for the analysis of complex systems," Phys. Rep. **438**, 237 (2007).
[46]Z.-K. Gao and Ning-De Jin, "A directed weighted complex network for characterizing chaotic dynamics from time series," Nonlin. Anal.: Real World Appl. **13**, 947 (2012).
[47]Z.-K. Gao, X.-W. Zhang, N.-D. Jin, N. Marwan, and J. Kurths, "Multivariate recurrence network analysis for characterizing horizontal oil-water two-phase flow," Phys. Rev. E **88**, 032910 (2013).
[48]J. W. Kantelhardta, S. A. Zschiegnera, E. Koscielny-Bundec, S. Havlind, A. Bundea, and H. Eugene Stanley, "Multifractal detrended fluctuation analysis of nonstationary time series," Physica A **316**, 87 (2002).
[49]Z.-K. Gao, X.-W. Zhang, N.-D. Jin, R. V. Donner, N. Marwan, and J. Kurths, "Recurrence networks from multivariate signals for uncovering dynamic transitions of horizontal oil-water stratified flows," Europhys. Lett. **103**, 50004 (2013).
[50]C.-K. Peng, S. Havlin, H. E. Stanley, and A. L. Goldberger, "Quantification of scaling exponents and crossover phenomena in nonstationary heartbeat time series," Chaos **5**, 82 (1995).
[51]B. Podobnik and H. Eugene Stanley, "Detrended cross-correlation analysis: A new method for analyzing two nonstationary time series," Phys. Rev. Lett. **100**, 084102 (2008).
[52]A. Bunde, S. Havlin, J. W. Kantelhardt, T. Penzel, J. Hermann Peter, and K. Voigt, "Correlated and uncorrelated regions in heart-rate fluctuations during sleep," Phys. Rev. Lett. **85**, 3736 (2000).
[53]Z.-K. Go and N.-D. Jin, "Scaling analysis of phase fluctuations in experimental three-phase flows," Physica A **390**, 3541 (2011).
[54]L. Muchnik, A. Bunde, and S. Havlin, "Long term memory in extreme returns of financial time series," Physica A **388**, 4145 (2009).